

2

## Polymers on graphite and gold: molecular images and substrate defects

by J. P. RABE, M. SANO‡, D. BATCHELDER\* and A. A. KALATCHEV†, *Max-Planck-Institut für Polymerforschung Postfach 3148, D-6500 Mainz, F.R.G.*

**KEY WORDS.** Scanning tunnelling microscopy, vibrational spectroscopy, Langmuir–Blodgett films, phthalocyaninato-poly-siloxane.

### SUMMARY

Sub-monomolecular layers of a derivatized Phthalocyaninato-poly-siloxane (PCPS) and a Polydiacetylene (PDA) have been prepared on highly orientated pyrolytic graphite and gold by Langmuir–Blodgett and Langmuir–Schäfer techniques. Raman scattering and grazing-incidence-reflection infrared spectroscopy were used to characterize packing and molecular orientations within these films. It was found that PCPS forms similarly well ordered monolayers on both graphite and gold while PDA does not. Scanning tunnelling microscopy (STM) was performed in air using both the constant height and constant current mode. On highly orientated pyrolytic graphite substrates various defect structures based on a  $\sqrt{3} \times \sqrt{3}$  R  $30^\circ$  superstructure were found near localized defects and small graphite steps. They were carefully distinguished from molecular images of densely packed hydrocarbon chains. Defect rich graphite was characterized with both STM and Raman spectroscopy. Similarly, disordered and graphite-like regions were found on carbon fibres. The sensitivity of STM to surface defects in graphitic material turned out to be large compared to that of the Raman spectroscopic method. STM images of PCPS monolayers on graphite and gold exhibited parallel polymer rods, 2 nm apart from each other.

### INTRODUCTION

Direct imaging of ultrathin organic films at molecular resolution is of considerable interest in the investigation of film microstructure, for example in Langmuir–Blodgett (LB) films (Möbius, 1988), or in the study of metal–polymer interfaces, for example in carbon fibre composites (Fitzer, 1984). Due to the very local character and its low energy, the STM probe (Binnig *et al.*, 1982, 1983) has a particular potential for the study of defects and disorder in both polymers and substrates. Recently, several STM studies have been devoted to ultrathin organic films on graphite (Rabe *et al.*, 1986a; Smith *et al.*, 1987; Hörber *et al.*, 1988; Braun *et al.*, 1988; Albrecht *et al.*, 1988; Foster & Frommer, 1988). However, all these studies were hampered by the difficulty to adhere an organic film onto graphite, a problem also known in the fabrication of carbon fibre composites. It was decided, therefore, to study first of all, possible adhesion sites in graphite, as there are steps, defects and disordered surface areas. Also, for comparison, gold

\* On leave from Queen Mary College, London, U.K.

† On leave from Institute of Petrochemical Synthesis of Acad. Sci. USSR, Moscow, USSR.

‡ Present address: RDC, Fukuoka, Japan.

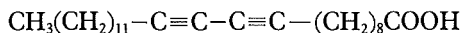
was used as a substrate. In an attempt to reduce the mobility of only loosely bound film molecules on the substrate, it was decided to use two polymeric materials for LB film formation: a derivatized Phthalocyaninato-poly-siloxane (PCPS) and a Polydiacetylene (PDA), which both form well-characterized LB multilayers on, for example, glass, silicon or gold (Lieser *et al.*, 1980; A. A. Kalatchev *et al.*, in preparation; T. Sauer *et al.*, in preparation). While PDA multilayers, much like the fatty acids, exhibit a crystalline hydrocarbon side chain packing, the PCPS molecules, in contrast, are rigid rods which are enclosed in a shell of short, flexible hydrocarbon side chains and which are lying flat on the substrate. Since the phthalocyanine cores are highly conjugated, the conductivity of PCPS is considerably larger than that of saturated hydrocarbons.

It turned out to be important to characterize any polymer film carefully with an independent method prior to its investigation with the STM. Grazing-incidence-reflection infrared spectroscopy and Raman scattering proved to be particularly powerful due to the high sensitivity of state-of-the-art instrumentation and the specific information they can provide.

#### EXPERIMENTAL

LB films were prepared on a commercially available film balance (Lauda, F.R.G.) using distilled and filtered water (Milli Q, Millipore Corporation).

The amphiphilic diacetylene



was transferred in the monomeric state to graphite substrates from a  $10^{-3}$  mol/l aqueous solution of  $\text{CdCl}_2$  (Lieser *et al.*, 1980). The pH was maintained at 6.5 through the addition of NaOH. The transfer pressure was 20 mN/m and the temperature 20°C. As observed earlier for cadmium arachidate on graphite, it was never possible to achieve a transfer ratio of better than  $\approx 70\%$  for the first monolayer, while transfer of about 100% was observed for the subsequent layers. In an attempt to improve the transfer of the first monolayer the following method was devised. First 4–6 layers of either diacetylene or a fatty acid salt (cadmium arachidate) were transferred onto graphite, then a narrow strip (1–2 mm wide) of graphite with the LB film on it was removed from the centre portion of the sample. The remaining layers surrounding the strip were supposed to serve as anchoring points for an additional LB transfer. Now either another monolayer (by dipping in through the free water surface and lifting through the monolayer) or a bilayer transfer was attempted.

Polymerization on the water surface or on the substrate was brought about by u.v.

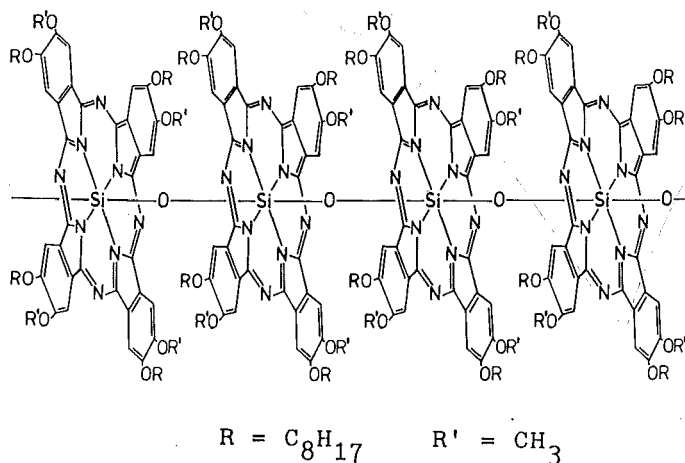


Fig. 1. Phthalocyaninato-poly-siloxane.

irradiation

$$\left( \lambda = 254 \text{ nm}, \quad \text{dose} = 3 \frac{\text{mW}}{\text{cm}^2} \text{ min} \right).$$

Monolayers prepolymerized on the water surface were transferred by both Langmuir–Blodgett and Langmuir–Schäfer techniques, that is vertical and horizontal dipping.

For gold substrates the usual LB method gave fairly good transfer also for the very first monolayer.

Derivatized Phthalocyaninato-poly-siloxane (Fig. 1) of molecular weight  $M_w = 62,500 \pm 5,000$ , corresponding to a weight average monomer number  $DP_w = 52 \pm 5$  was prepared by T. Sauer (Sauer & Wegner, 1988; Caseri *et al.*, 1988). Good quality LB layers were obtained from a clean water subphase at a temperature of 6°C (A. A. Kalatchev *et al.*, in preparation). With a transfer pressure of 25 mN/m and a dipping speed of 10 mm/min the transfer ratio was close to unity. Some samples were annealed after transfer at 160°C for 6 days. Also some samples were treated by iodine vapour for 30 s.

The substrate material mostly used throughout this study was highly orientated pyrolytic graphite (HOPG), donated by Dr A. Moore (Union Carbide, U.S.A.). For comparison, 100 nm thick gold films evaporated onto glass slides were used.

STM images were obtained with an instrument developed for fast and stable operation in gases and liquids. The scanner was a single piezoelectric tube (EBL Company, U.S.A.) (Binnig & Smith, 1986) with a scan range of 1.5  $\mu\text{m}$ . Coarse sample approach was brought about by a differential micrometer (Fig. 2). The STM head was placed in an evacuable bell jar onto a stack of metal plates separated by viton spacers. The bell jar together with an adsorption pump was mounted on an optical table supported by an air spring vibration isolation system (Newport, U.S.A.). The STM electronics allowed for both the constant current (Binnig *et al.*, 1982) and the constant height mode (Bryant *et al.*, 1986). In the former case data acquisition was performed with an IBM PC/AT. In the latter the tip was scanned with 1 kHz in the  $x$ -direction

Piezo Tube – Scanner                      Tip                      Sample                      Micrometer

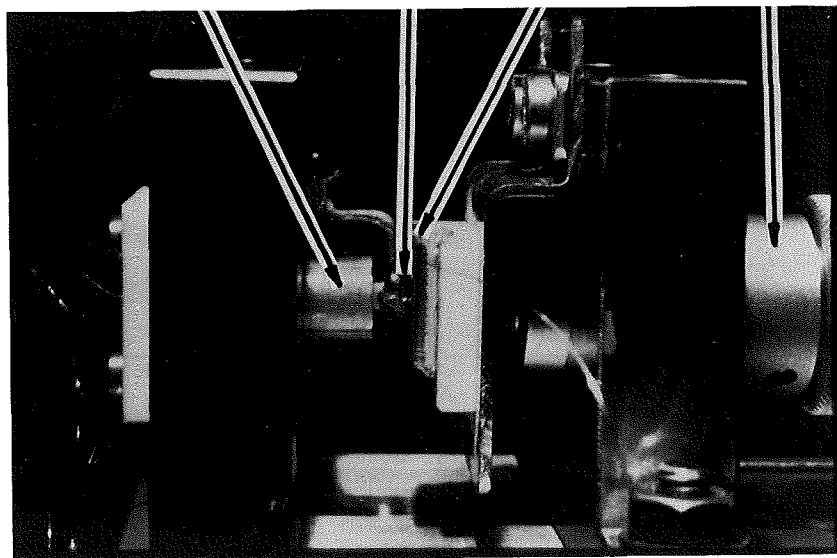


Fig. 2. STM Head.

and 40 Hz in the  $y$ -direction and the current signal was transformed into a video image by an image processor (Arlunya TF 6540) and stored on video tape. A number of frames could then be averaged or digitized for further digital image processing. The tips used were mostly mechanically sharpened Pt/Ir and occasionally electrochemically etched W (2-n-NaOH, 12 V ac). The tunnelling current was generally 2 nA. All images presented in this paper were obtained at ambient conditions.

Grazing-incidence-reflection FT-IR experiments were performed with a Nicolet 60 SX spectrometer, equipped with a narrow band HgCdTe detector. The angle of incidence was  $80^\circ$ . Details of the set-up are given elsewhere (Arndt & Bubeck, 1988). The method has proven valuable in the determination of microstructure in polymeric LB films on highly reflecting substrates (Rabe *et al.*, 1986b). Its extension to less reflecting substrates like graphite is also possible, however, and will be discussed elsewhere (J. P. Rabe, in preparation).

Raman spectra on graphite steps were obtained with an Ar-ion laser (Coherent Innova 90), a Triplemonochromator (Spex 1877) and a CCD camera detection system (Wright Instruments). The 514 nm laser line was used with about 800 mW power at the sample. The angle of incidence was about  $30^\circ$  and the Raman scattered light was collected under an angle of about  $60^\circ$ . Spectrum acquisition time was about 20 min. Raman spectra of the PDA films were obtained with a photomultiplier.

### RESULTS AND DISCUSSION

In order to address the question of adhesion of the first LB monolayer and the role of surface defects, an HOPG sample full of small steps was investigated. Figure 3 shows constant current STM plots of individual mono- and bilayer steps; a disordered region around a monostep and a typical scan along a  $1.5\ \mu\text{m}$  long strip indicating the distribution of steps and surface disorder for this particular sample. The area fraction of the disordered surface is of the order of 20%.

On the same sample, Raman spectra have been obtained in order to find a correlation between the STM data and the intensity of a band at  $1355\ \text{cm}^{-1}$ , not found in single crystalline graphite and attributed to finite crystallite size in disordered graphite (Tuinstra & Koenig, 1970; Nemanich & Solin, 1979). Due to the absorption of light in graphite, the Raman signal originates from a thin penetration layer near the surface. While on flat high quality HOPG no indication of the  $1355\ \text{cm}^{-1}$  line was observed, a weak contribution was found on the stepped surface (Fig. 4). However, it never exceeded about 1% of the intensity of the allowed peak at  $1580\ \text{cm}^{-1}$ , indicating that it is still a fairly well ordered sample compared to glassy carbon (Tuinstra & Koenig, 1970; Nemanich & Solin, 1979). This means on the other hand that STM is very sensitive to surface disorder if compared to the Raman method.

In this context it may be worthwhile to note that the surface of carbon fibres can be investigated in the same fashion. Indeed, Raman spectroscopy can be applied to characterize

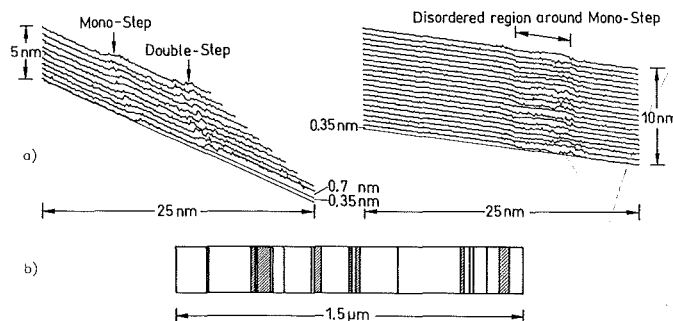


Fig. 3. (a) STM images of mono- and bilayer steps on graphite in the constant current mode. (b) Top view representation of steps and disordered regions (hatched) in an HOPG sample full of steps.

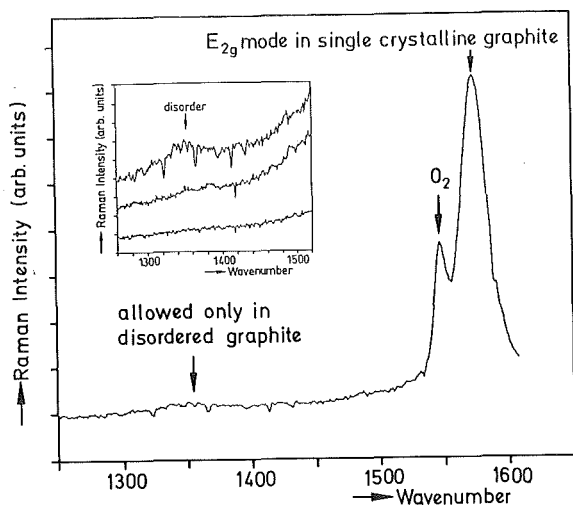


Fig. 4. Raman spectra at different spots of the same stepped sample investigated by STM (Fig. 3). Nowhere on the sample did the intensity of the band at  $1355\text{ cm}^{-1}$  exceed 1% of the band at  $1580\text{ cm}^{-1}$ .

surface modification of carbon fibres and, on the other hand, Fig. 5 shows that the intrinsic conductivity of the pure carbon fibre is large enough to allow for direct STM imaging with a resolution of about  $0.2\text{ nm}$ .

High resolution imaging of HOPG near small steps and defects revealed two common types of superstructures: a  $\sqrt{3}\times\sqrt{3}$  R  $30^\circ$  structure of bright spots as well as one of the dark spots or, alternatively speaking, of bright rings (Fig. 6). The intensity of both superstructures relative to the graphite lattice decays away from the defect or step over some ten lattice constants. In some cases the superstructure near the defect may be so strong that it dominates the image.

A superstructure of the first type (Fig. 6b) has been calculated by H. A. Mizes and J. S.

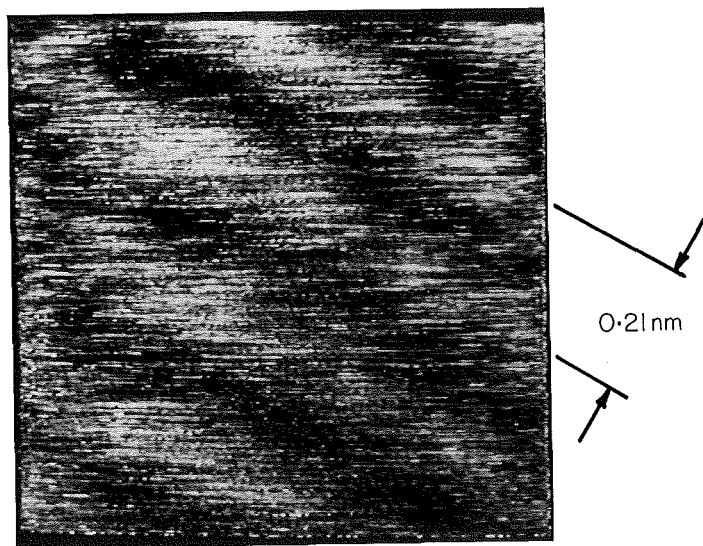
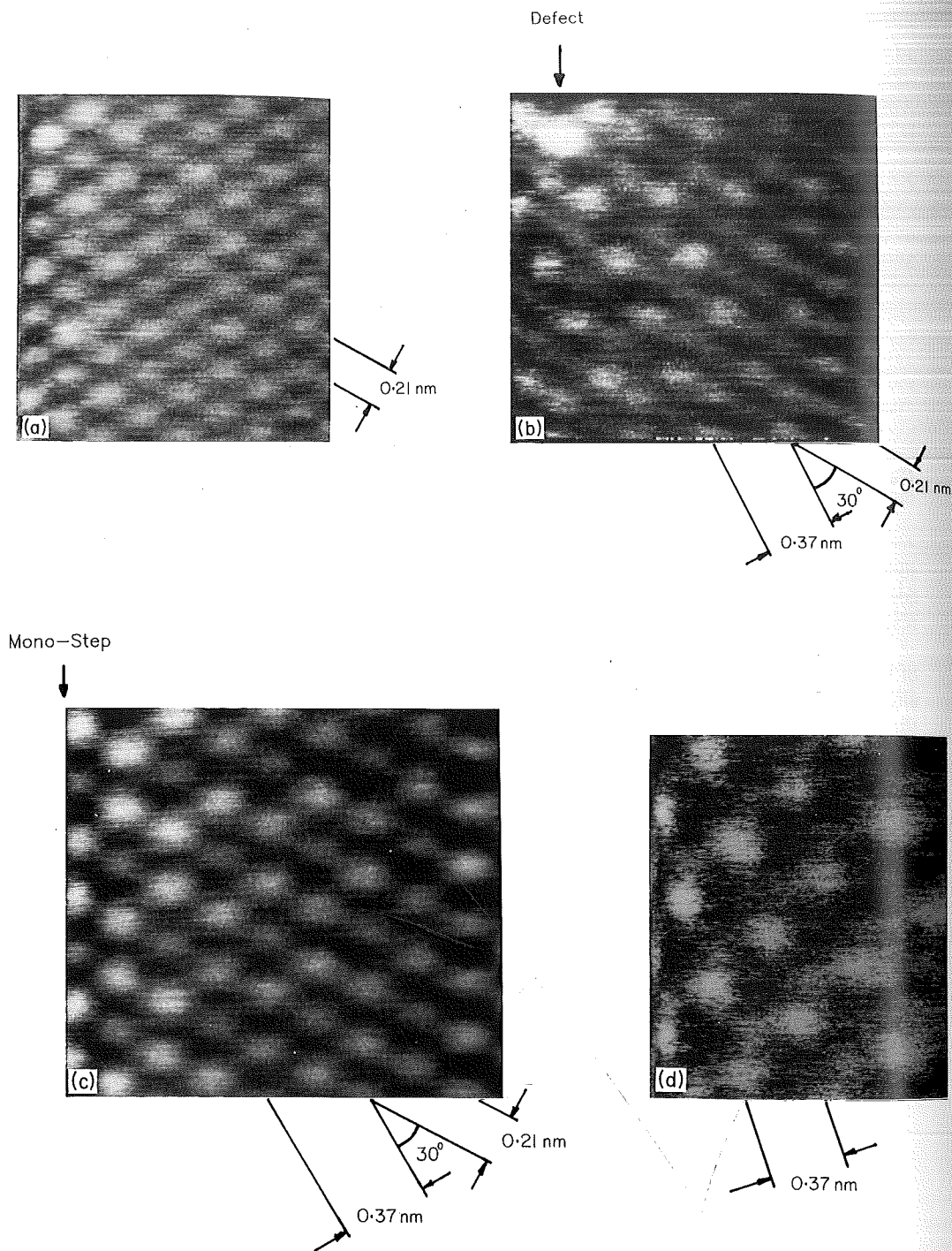


Fig. 5. High resolution STM image of a carbon fibre. Separation between two rows is  $0.21\text{ nm}$ .



**Fig. 6.** STM images in the constant height mode. (a) Highly orientated pyrolytic graphite. (b)  $\sqrt{3} \times \sqrt{3}$  R  $30^\circ$  superstructure near localized defect on graphite. (c) Inverse  $\sqrt{3} \times \sqrt{3}$  R  $30^\circ$  structure next to graphite step. (d)  $\sqrt{3} \times \sqrt{3}$  R  $30^\circ$  structure dominating STM image close to a defect. Intensity of superstructure relative to graphite image decays away from the defect over some 3 nm.

Foster (unpublished observations) as a consequence of an electronic perturbation of the graphite due to a point defect, like a vacancy or a bond to an adsorbant. The second type (Fig. 6c) could, for example, be attributed to a superposition of two superstructures of the first type shifted relative to each other. It was less often observed.

Another  $\sqrt{3} \times \sqrt{3} R 30^\circ$  structure near a step is shown in Fig. 7. In this case the superstructure extends over not more than three lattice constants and then disappears abruptly, clearly different from those in Fig. 6. It should be noted that in this case the sample had been dipped through a PDA monolayer in an attempt to transfer an LB film. However, on most of the sample pure graphite images were obtained. Also, the superstructures in Fig. 7 are unlikely to

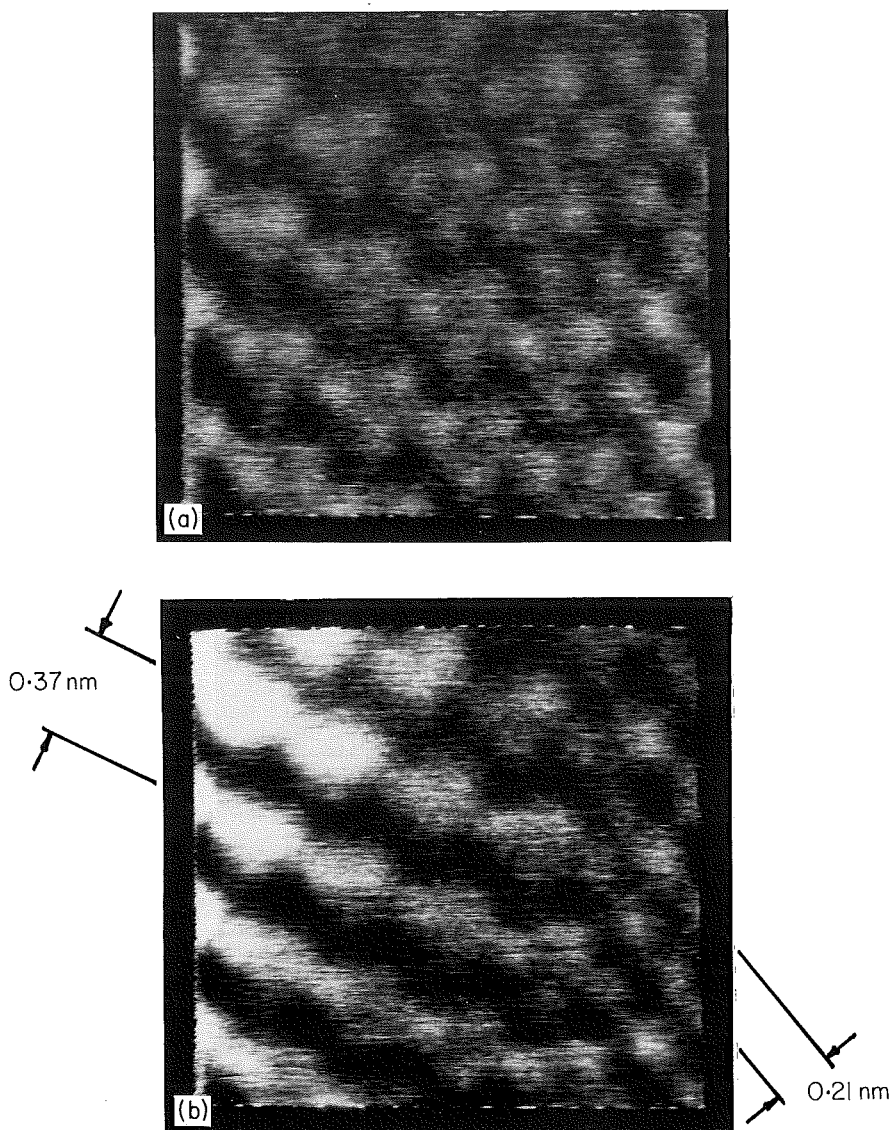


Fig. 7. STM images in the constant height mode. (a)  $\sqrt{3} \times \sqrt{3} R 30^\circ$  structure composed of triplets next to the graphite step. In this case there is a sharp transition to the graphite image. (b) If smeared out again, a  $\sqrt{3} \times \sqrt{3} R 30^\circ$  superstructure appears next to the graphite.

be an image of the densely packed hydrocarbon side chains of PDA, adsorbed at the step. Reasons for this conclusion are first of all that the constant current images of the step did not reveal a step of about 2.5 nm in height but rather a fairly clean monostep in graphite and second that triplets can be resolved in each element of the superlattice. Moreover, in contrast to earlier reports on molecular images on LB films, no drift or motion of the structure relative to graphite was observed. This structure is, therefore, more likely a graphite defect. Since it occurs on the higher side of the step, it is possibly associated with some ions intercalated from the edge.

Since monitoring of the PDA monolayer transfer with the film balance indicated the difficulties in transferring the very first monolayer, the state of this monolayer after transfer was investigated by resonance Raman spectroscopy. This investigation could be performed on the same sample examined later with FT-IR and STM. The band at  $1451\text{ cm}^{-1}$ , assigned to the carbon double bond stretch vibration (Tieke & Bloor, 1979), was used as an indication of the presence of the well ordered, so-called blue polymer phase. Using a laser wavelength of 647 nm, it was found that the intensity of this Raman band divided by the number of monolayers dropped to 50% in going from 20 to 10 monolayers and was at best 10% for a mono- or a bilayer. This means that even despite a fairly good transfer, that is the case of the preformed polymer layer transferred on the partially precoated substrate, we were not able to prepare the well ordered blue phase of PDA films on graphite. This conclusion was further evidenced by FT-IR measurements which showed that the hydrocarbon chains on graphite were orientated very differently (much more parallel to the substrate) than on gold.

STM experiments on PDA mainly gave graphite images except on one sample which was covered over large areas by a superstructure of about 1 nm periodicity present at the same time as the graphite lattice. The PDA Raman band for this sample was particularly strong and the

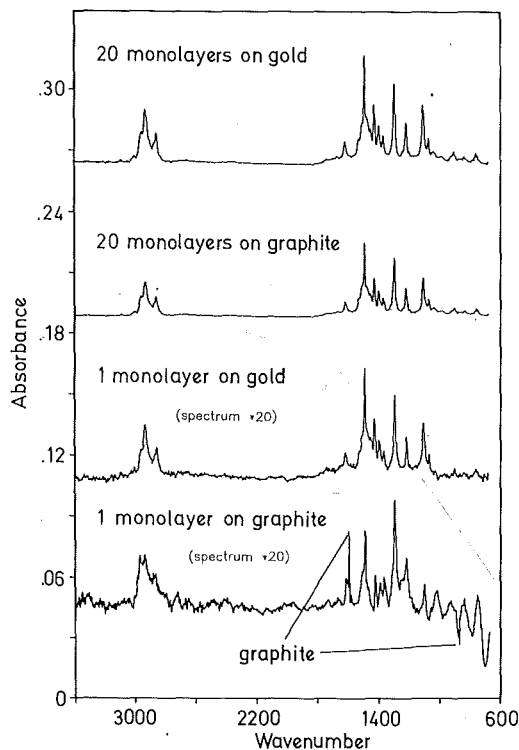


Fig. 8. Grazing-incidence-reflection infrared spectra of one and twenty monolayers on graphite and gold.

STM image was obtained very reproducibly for this sample; however, the preparation could not be reproduced. Hence no reproducible STM image of PDA on graphite has been obtained.

The transfer of the Phthalocyaninato-poly-siloxane (PCPS) onto gold and graphite was more reproducible than for PDA. From the grazing-incidence-reflection FT-IR spectra (Fig. 8) it can be concluded that twenty monolayers on gold and graphite and one monolayer on gold are structurally identical while one monolayer on graphite is at least similar. Together with the bulk and transmission spectra and the bond assignments (Sauer *et al.*, 1988), the following picture emerges for a monolayer on gold and graphite: the rigid polymer rods are lying flat on the substrate with their long axes aligned preferentially along the dipping direction. The layer

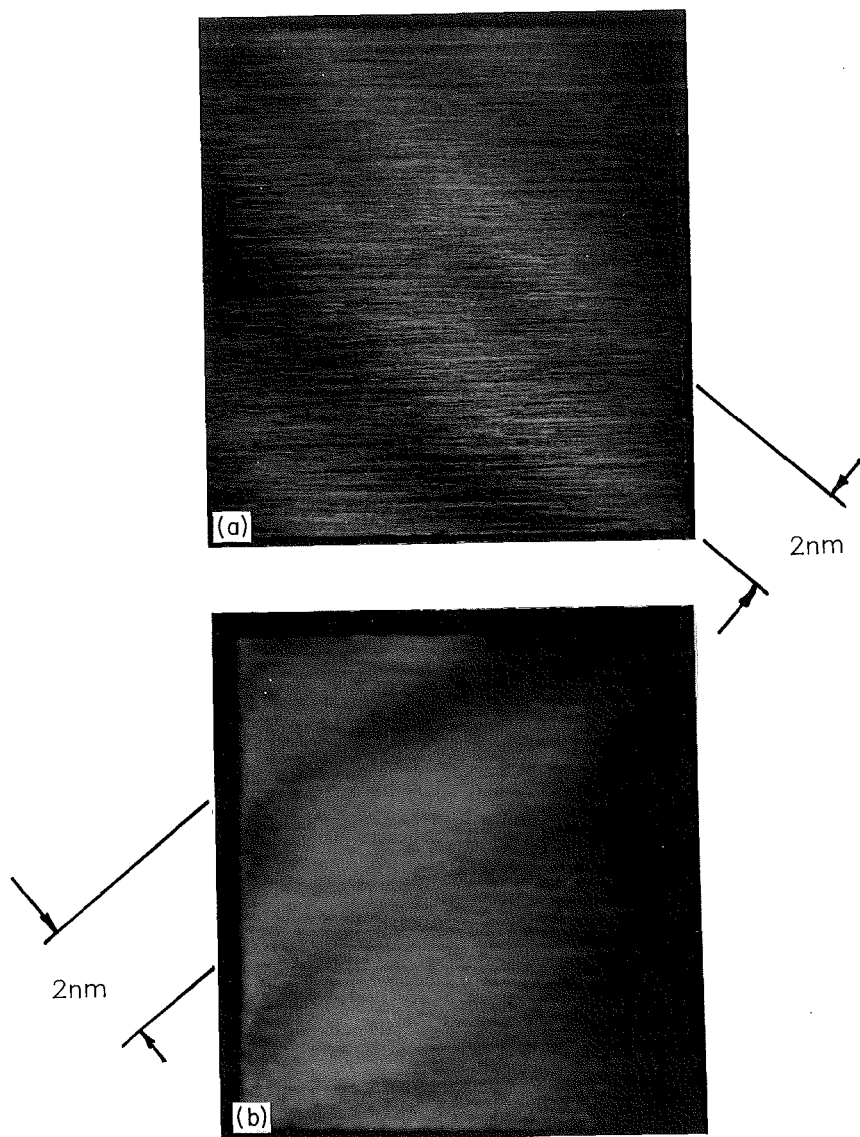


Fig. 9. Phthalocyaninato-poly-siloxane on (a) graphite and (b) gold. The graphite sample had been annealed at 160°C for 6 days. The gold sample had been treated with iodine vapour for 30 s.

spacing in multilayers, as determined by X-ray diffraction (Sauer *et al.*, 1988), is 2 nm, in good agreement with the diameter of the rods.

STM images of PCPS graphite and gold are given in Fig. 9. Areas with parallel rods, about 2 nm apart, are found on both substrates, gold and graphite. No structure along the rods could be resolved and the stripes would somewhat jiggle around, though the position of any individual rod could be clearly followed on the video recording.

This behaviour can be understood since the flexible side chains attached to the phthalocyanine rings prevent any strong interaction of the polymer either to the substrate or to neighbouring molecules; that is, the polymer rods may slide past each other or rotate around their long axes but, due to their form anisotropy, the rods will remain parallel to each other.

#### CONCLUSION

Among various defect structures observed on highly orientated pyrolytic graphite, it is in particular a  $\sqrt{3} \times \sqrt{3}$  R 30° superstructure which is repeatedly found near localized defects and small steps. Defects on graphite and carbon fibres, which can be investigated with both STM and Raman spectroscopy, have been carefully distinguished from molecular images of deposited polymer films. The successful imaging of PCPS molecules on graphite and gold is ascribed partly to the good film quality if compared to PDA. It should be noted again, however, that for the PCPS films on graphite, some considerable fraction of the sample exhibits clean graphite images, indicating that also PCPS does not form perfect, adhering monolayers on graphite. Clearly, the search for alternative substrates should be continued.

#### ACKNOWLEDGMENTS

It is a pleasure to acknowledge T. Sauer for providing us with the Phthalocyaninato-poly-siloxane, A. Moore for the graphite, H. Knobloch and T. Arndt for part of the Raman and infrared spectra and M. Pohlmann for his technical assistance in building the STM. Also we would like to thank J. S. Foster and H. A. Mizes for a preprint of their work. This project has been funded by the Bundesministerium für Forschung und Technologie under the title Ultrathin Layers of Polymers, 03M4008E9.

#### REFERENCES

- Albrecht, T.R., Dovek, M.M., Lang, C.A., Grütter, P., Quate, C.F., Kuan, S.W.J., Frank, C.W. & Pease, R.W.F. (1988) Imaging and modification of polymers by scanning tunneling and atomic force microscopy. *J. Appl. Phys.* **64**, 1178–1184.
- Arndt, T. & Bubeck, Ch. (1988) Fourier transform IR spectroscopy of protonated cadmium arachidate layers in different positions of a perdeuterated multilayer. *Thin Solid Films*, **159**, 443–449.
- Binnig, G., Rohrer, H., Gerber, Ch. & Weibel, E. (1982) Surface studies by scanning tunneling microscopy. *Phys. Rev. Lett.* **49**, 57–61.
- Binnig, G., Rohrer, H., Gerber, Ch. & Weibel, E. (1983) 7×7 reconstruction on Si (111) resolved in real space. *Phys. Rev. Lett.* **50**, 120–123.
- Binnig, G. & Smith, D.P.E. (1986) Single-tube three dimensional scanner for scanning tunneling microscopy. *Rev. Sci. Instrum.* **57**, 1688–1689.
- Braun, H.G., Fuchs, H. & Schrepp, W. (1988) Surface structure investigation of Langmuir Blodgett-films. *Thin Solid Films*, **159**, 301–314.
- Bryant, A., Smith, D.P.E. & Quate, C.F. (1986) Imaging in real time with the tunneling microscope. *Appl. Phys. Lett.* **48**, 832–834.
- Caseri, W., Sauer, T. & Wegner, G. (1988) Soluble phthalocyaninato-poly-siloxanes: rigid rod polymers of high molecular weight. *Makromol. Chem., Rapid Commun.* **9**, 651–657.
- Fitzer, E. (ed.) (1984) *Carbon Fibres and their Composites*, Springer-Verlag, Berlin.
- Foster, J.S. & Frommer, J.E. (1988) Imaging of liquid crystals using a tunneling microscope. *Nature*, **333**, 542–545.
- Hörber, J.K.H., Lang, C.A., Hänsch, T.W., Heckl, W.M. & Möhwald, H. (1988) Scanning tunneling microscopy of lipid films and embedded biomolecules. *Chem. Phys. Lett.* **145**, 151–158.
- Lieser, G., Tieke, B. & Wegner, G. (1980) Structure, phase transitions and polymerizability of multilayers of some diacetylene monocarboxylic acids. *Thin Solid Films*, **68**, 77–90.
- Möbius, D. (ed.) (1988) *Thin Solid Films*, pp. 159–160.

- Nemanich, R.J. & Solin, S.A. (1979) First- and second-order Raman scattering from finite-size crystals of graphite. *Phys. Rev. B*, **20**, 392-401.
- Rabe, J.P., Gerber, Ch., Swalen, J.D., Smith, D.P.E., Bryant, A. & Quate, C.F. (1986a) An image of a lipid bilayer at molecular resolution by scanning tunneling microscopy. *Bull. Am. Phys. Soc.* **31**, 289.
- Rabe, J.P., Rabolt, J.F., Brown, C.A. & Swalen, J.D. (1986b) Order-disorder transitions in Langmuir Blodgett films II. IR studies of the polymerization of Cd-octadecylfumarate and Cd-octadecylmaleate. *J. Chem. Phys.* **84**, 4096-4102.
- Sauer, T. & Wegner, G. (1988) Control of the discotic to isotropic transition in alkoxy-substituted silicon-dihydroxo-phthalocyanines by axial substituents. *Mol. Cryst. Liq. Cryst.* **162B**, 97-118.
- Smith, D.P.E., Bryant, A., Quate, C.F., Rabe, J.P., Gerber, Ch. & Swalen, J.D. (1987) Images of a lipid bilayer at molecular resolution by scanning tunneling microscopy. *Proc. Natl. Acad. Sci. USA*, **84**, 969-972.
- Tieke, B. & Bloor, D. (1979) Raman spectroscopic studies of the solid-state polymerization of diacetylenes, 3. UV-polymerization of diacetylene Langmuir-Blodgett multilayers. *Makromol. Chem.* **180**, 2275-2278.
- Tuinstra, F. & Koenig, J.L. (1970) Raman spectrum of graphite. *J. Chem. Phys.* **53**, 1126-1130.